INTEGRATING NEAREST NEIGHBORS WITH NEURAL NETWORK MODELS FOR TREATMENT EFFECT ESTIMATION

A PREPRINT

Niki Kiriakidou*
Department of Informatics and Telematics,
Harokopio University of Athens,
Athens, GR177 78.
kiriakidou@hua.gr

Christos Diou
Department of Informatics and Telematics,
Harokopio University of Athens,
Athens, GR177 78.
cdiou@hua.gr

June 22, 2023

ABSTRACT

Treatment effect estimation is of high-importance for both researchers and practitioners across many scientific and industrial domains. The abundance of observational data makes them increasingly used by researchers for the estimation of causal effects. However, these data suffer from several weaknesses, leading to inaccurate causal effect estimations, if not handled properly. Therefore, several machine learning techniques have been proposed, most of them focusing on leveraging the predictive power of neural network models to attain more precise estimation of causal effects. In this work, we propose a new methodology, named Nearest Neighboring Information for Causal Inference (NNCI), for integrating valuable nearest neighboring information on neural network-based models for estimating treatment effects. The proposed NNCI methodology is applied to some of the most well established neural network-based models for treatment effect estimation with the use of observational data. Numerical experiments and analysis provide empirical and statistical evidence that the integration of NNCI with state-of-the-art neural network models leads to considerably improved treatment effect estimations on a variety of well-known challenging benchmarks.

Keywords Causal inference · treatment effects · performance profiles · non-para-metric tests · post-hoc tests

1 Introduction

Causal effect estimation is often the central research data analysis objective across many scientific disciplines. In particular, it is the process of inferring a causal relationship between an intervention, or else treatment, and its effect on an outcome variable of interest. It involves quantifying the extent to which a change in a given intervention or treatment would influence the variable of interest. Among others, treatment effect is used in healthcare Schneeweiss et al. (2009),Zheng et al. (2022), education Oreopoulos (2006) and advertising Zantedeschi et al. (2017). Some examples of causal questions in each one of these fields include "*What is the effect of a specific drug on a patient's blood pressure levels?*", "*What is the effect of studying two more hours on a student's final test performance?*", "*What is the effect of an advertisement on social media to the product's sales?*", respectively.

The golden standard for answering these questions is through the conduction of Randomized Controlled Trials (RCTs), in which subjects are randomly assigned to two groups: the *treatment group* (also known as intervention or experimental) and the *control group*. The intervention of interest is applied on the members of the treatment group, while no intervention is applied on the members of the control group. Due to randomization, RCTs enable the calculation of the real treatment effect. Nevertheless, in most of the cases it is impossible to conduct an RCT due to financial and/or ethical issues, or due to the large number of combinations of variables that need to be evaluated.

---

*Corresponding author.

Therefore, researchers from various high-impact scientific areas could be benefited from the plethora of readily available observational data for the estimation of treatment effects. Nevertheless, handling observational data enclose several complications Kuang et al. (2020); Hammerton and Munafò (2021), since actions and outcomes are observed retrospectively and the mechanism caused the action is unknown. Additionally, observational data may include possible (hidden or observed) counfounding variables, which lead to incorrect estimation of treatment effects. Hence, there has been a growing interest in using machine learning models for causal effect estimation, as these models can leverage observational data as well as they can capture complex relationships between variables and provide accurate predictions.

In this work, we propose a new methodology for integrating information from neighboring samples in neural network architectures for treatment effect estimation. The proposed methodology, named Nearest Neighboring Information for Causal Inference (NNCI), is implemented on the most effective neural network-based models, which provide predictions of the outcomes from control and treatment groups as well as for the propensity score, i.e., the probability for a subject to be assigned into the treatment group. The motivation of our approach consists of enriching the models' inputs with valuable information from control and treatment groups along with the covariates in order to improve the estimations of treatment effects. The proposed methodology identifies the nearest neighbor instances in the control group and the treatment group for each instance and then calculates the average outcomes of identified instances contained in both groups. This information is integrated with the covariates to the model's inputs in order to increase the prediction accuracy and reduce bias. By using the outcomes of the nearest neighbors as input features, the methodology aims to capture the causal effects of the treatment more efficiently. The neural network models can learn to weight these new input features appropriately, and better capture complex relationships between the features and the treatment effect. Summarizing, the main contributions of this work are:

- NNCI methodology for integrating information from neighboring instances in neural network-based causal inference models for treatment effect estimation.
- the modification of the architecture of three state-of-the-art neural network models i.e., Dragonnet Shi et al. (2019), TARnet Shalit et al. (2017) and NEDnet Shi et al. (2019) for incorporating the information provided by NNCI. The developed models use a vector of features extracted from the outcomes of the nearest neighbors of each sample, separately for the treatment and control group as inputs, to improve treatment effect estimation.
- a comprehensive experimental analysis based on Dolan and Moré (2002) performance profiles as well as on post-hoc and non-parametric statistical tests Finner (1993); Hodges Jr and Lehmann (1962). The conducted analysis demonstrate that in most cases the proposed methodology leads to considerable improvement in the estimation of treatment effects, while in a minority of the cases, it exhibits similar performance with the corresponding baseline model.

The remainder of this paper is organized as follows: Section 2 presents a brief review of the state-of-the-art baseline models for treatment effect estimation. Section 3 presents a detailed description of the proposed methodology and the proposed neural network-based models in which NNCI methodology is adopted. Section 4 presents the used datasets and the evaluation methodology. Section 5 presents the numerical experiments, focusing on the evaluation of the proposed neural network-based causal inference models with the corresponding baseline models. Section 6 discusses the proposed framework as well as the experimental results and outlines the findings of this work. Finally, Section 7 summarizes the main findings and conclusions of this work as well as some interesting directions for future work.

2 Related Work

In recent years, researchers aimed at leveraging machine learning models for treatment effect estimation from observational data. Neural networks have demonstrated that they offer high capacity, while at the same time avoiding overfitting for a range of applications, including representation learning. Therefore, there has been considerable interest in using them for the estimation of causal effects at both the individual and population level. Next, we briefly describe the most well-mentioned.

Yoon et al. Yoon et al. (2018) proposed a new causal inference model, named Generative Adversarial Nets for the inference of Individualized Treatment Effects (GANITE) for estimating individual treatment effects. The rationale of their approach was the simulation of uncertainty regarding the counterfactual distributions, which was achieved by learning these distributions using a GAN model. The presented numerical experiments revealed that GANITE outperformed S-learner machine learning models Künzel et al. (2019) as well as some tree-based models (BART Chipman et al. (2010), R-Forest Breiman (2001) and C-Forest Wager and Athey (2018)) on three benchmarks.

Louizos et al. (2017) proposed Causal Effect Variational Auto-Encoder (CEVAE), for leveraging the proxy variables for the accurate estimation of treatment effects. The main advantage of the CEVAE is that it requires substantially weaker assumptions about the structure of the hidden confounders as well as about the data generating process. The authors

provided a comprehensive experimental analysis, which presented that CEVAE exhibited better performance compared to traditional causal inference models and presented more robust behavior against hidden confounders in the case of noisy proxies.

Shalit et al. (2017) proposed a new framework, named Counterfactual Regression (CFR), which focuses on learning a balanced representation of treatment and control groups using a prediction model. The authors utilized two distances, namely Maximum Mean Discrepancy (MMD) Gretton et al. (2012) and Wasserstein distance (Wass) Villani (2009) to measure the distances between treatment and control groups' distributions. In addition, they proposed Treatment Agnostic Representation Network (TARnet) neural network model, which constitutes a variant of CFR without balance regularization. The experimental analysis revealed the superiority of TARnet and CFR (Wass) over S-learner and tree-based causal inference models.

Recently, Shi et al. (2019) proposed a three-head neural network model, named Dragonnet for the estimation of conditional outcomes as well as the propensity score and a new loss function, named *targeted regularization* for further improving the estimation of causal effects and reduce the bias of the estimator. Furthermore, the authors proposed a modification of Dragonnet, named NEDnet, which was trained with a multi-stage procedure instead of an end-to-end. The main difference is that NEDnet is first trained using a pure treatment prediction objective, which is then replaced with an outcome-prediction matching (three-head), similar to the one used by Dragonnet. The representation layers are then frozen and the outcome-prediction neural network is trained on the pure outcome prediction task. The reported experimental results showed that both Dragonnet and NEDnet achieved to get better estimations than the state-of-the-art models and concluded that both models along with targeted regularization substantially improve estimation quality.

Kiriakidou and Diou Kiriakidou and Diou (2022a) proposed a neural network causal inference model, named modified Dragonnet. The proposed model captures information not only from covariates, but also from the average outcomes of neighboring instances from both treatment and control groups. For evaluating the efficiency of their approach, they used the semi-synthetic collection datasets IHDP Hill (2011). In their experiments, the proposed model was implemented with three different Minkowski distance metrics for the calculation of neighboring instances. The presented experimental analysis revealed that modified Dragonnet constitutes a better estimator than Dragonnet for all utilized metrics, while simultaneously is able to predict treatment effects with high accuracy. Nevertheless, the limitation of this approach was that the authors adopted the proposed approach on one neural network-based causal inference model and that the evaluation was based only on one benchmark.

In this research, we present an extension of our previous work Kiriakidou and Diou (2022a) by proposing a new methodology, named Nearest Neighboring Information for Causal Inference (NNCI), based on the exploitation of valuable information provided by nearest neighboring instances-based philosophy for each instance. NNCI is applied on the most well-established neural network-based causal inference models proposed in the literature, namely Dragonnet, TARnet and NEDnet for capturing the causal effect estimations more accurately. Notice that these models were selected due to their special architecture design and the fact that they constitute the only neural network-based model to provide estimations for the propensity score as well as the conditional outcomes for control and treatment groups. The major difference between the presented works and the proposed approach is that the former ignore valuable information contained in the outcomes of the training instances; while the latter enriches the models' inputs with information from the covariates as well as from the outcomes from the control group and the treatment group. The main idea of the proposed approach is that the neural network causal inference models, through the adoption of NNCI are able to better capture complex causal relationships between the features and the treatment effect by appropriately weighting the advanced input features. Furthermore, in contrast to the usual approach for the performance evaluation of models for treatment effect estimation Yao et al. (2018); Shi et al. (2019); Johansson et al. (2016); Shalit et al. (2017); Louizos et al. (2017), we provide concrete and empirical evidence about the superiority of our approach, by using Dolan and Moré's Dolan and Moré (2002) performance profiles and a detailed statistical analysis based on non-parametric and post-hoc statistical tests Hodges Jr and Lehmann (1962); Finner (1993).

3 Methodology

In this section, we provide a detailed presentation of the proposed methodology for treatment effect estimation. We recall that the rationale behind our approach is to exploit the wealth of information from nearest neighboring instances from the training data in order to get more accurate estimations of average and individual treatment effects. This is achieved through the enrichment of model's inputs with the average outcomes of the nearest neighbors from the control and treatment groups of each instance contained in the training data.

3.1 Problem setup

In this work, we are relying on the potential outcome framework of Neyman-Rubin Rubin (2005). We consider a d-dimensional space of covariates X and a joint distribution Π on $\mathcal{X} \times \mathcal{T} \times \mathcal{Y}$, where $\mathcal{X}$, $\mathcal{T}$ and $\mathcal{Y}$ are the domains of random variables corresponding to the covariates, the treatment and the outcome of a sample, respectively.

According to the potential outcome framework we can learn causal effects given on a set of treatment-outcome pairs (T, Y). Throughout the paper, we are considering the case of binary treatment, which means that $T \in \{0, 1\}$, where $T = 0$ and $T = 1$ corresponds to the samples belong to the control and treatment group, respectively. Notice that for every instance i, there is a potential outcome $y_i^{(T)}$: $y_i^{(0)}$ for the samples belong to the control group and $y_i^{(1)}$ for the samples belong to the treatment group. It is worth mentioning that the fundamental problem of causal inference is that only one of the potential outcomes can be observed for each instance. In case the sample belongs to the treatment group, then $y_i^{(1)}$ is the factual outcome and $y_i^{(0)}$ is the counterfactual outcome, and vice-versa for samples belong to the control group.

Treatment effects can be defined using the potential outcomes $y_i^{(0)}$ and $y_i^{(1)}$. One of the causal effects we are interested to estimate is the *Individual Treatment Effect* (ITE), which measures the effect of the treatment on a single sample:

$$\text{ITE}_i = y_i^{(1)} - y_i^{(0)} \tag{1}$$

To measure the causal effect of a treatment over the whole population, we use the *Average Treatment Effect* (ATE):

$$\text{ATE} = E[Y \mid T = 1] - E[Y \mid T = 0] \tag{2}$$

Finally, for measuring the treatment effect for a specific subgroup of the population, i.e., samples with a specific value to the covariates X, we estimate the *Conditional Average Treatment Effect* (CATE):

$$\text{CATE}(\mathbf{x}) = E[Y \mid X = \mathbf{x}, T = 1] - E[Y \mid X = \mathbf{x}, T = 0] \tag{3}$$

A standard dataset for inferring treatment effect consists of the covariate matrix $\mathbf{X}$, the treatment vector $\mathbf{t}$ and the outcome vector $\mathbf{y}$.

3.2 Nearest neighboring information for causal inference

The proposed Nearest Neighboring Information for Causal Inference (NNCI) methodology aims to enrich the inputs of neural network models with information from nearest neighboring instances, to estimate treatment effects from observational data. More specifically, for each instance $\mathbf{x}_i$, NNCI identifies its k nearest neighboring instances in the control and treatment groups. Then, we calculate the average outcomes of the identified instances from both groups. These quantities, denoted as $\overline{y}_i^{(0)}$ and $\overline{y}_i^{(1)}$, are incorporated as additional input features to the neural network models. By using the outcomes of the nearest neighbors $\overline{y}_i^{(0)}$ and $\overline{y}_i^{(1)}$ as input features, the NNCI methodology aims to capture the effect of the intervention more efficiently. The neural network models can learn to weight these new input features appropriately; hence, to better capture complex relationships between the features and the treatment effect.

NNCI is integrated to the most effective neural network-based causal inference models i.e. Dragonnet, TARnet and NEDnet due to their special architecture design. More analytically, these models use a deep net to produce a representation layer, which is then processed independently for predicting both the outcomes for treatment and control groups. The adoption of NNCI to these models has the result of using as inputs the instance $\mathbf{x}_i = (\mathbf{x}_{i_1}, \mathbf{x}_{i_2}, \cdots, \mathbf{x}_{i_n})$ contained in the covariate matrix $\mathbf{X}$ along with the average outcomes of the neighboring instances from treatment and control groups, $\overline{y}_i^{(1)}$ and $\overline{y}_i^{(0)}$, respectively, as it is presented in Figure 1.

Algorithm 1 presents the pseudocode of NNCI methodology for calculating information from the outcomes of the instances contained in the training data. The inputs are the selected number of nearest neighbors k, the covariate matrix $\mathbf{X}$, the binary vector of treatment values $\mathbf{t}$ and the vector with the outcome values $\mathbf{y}$. The outputs are the vectors $\overline{\mathbf{y}}^{(0)}$ and $\overline{\mathbf{y}}^{(1)}$, containing the average values of neighboring outcomes for each sample from control and treatment group, respectively.

In Step 1, $\mathbf{y}^{(0)}$ and $\mathbf{y}^{(1)}$ are set to $\mathbf{0}$. For every instance $\mathbf{x}_i$, NNCI calculates the average values of neighboring outcomes from the control and treated groups (Steps 2-7). In more detail, in Step 4, NNCI calculates the k-nearest neighbors of instance $\mathbf{x}_i$, which belong in the control group (i.e $T = 0$) and store their corresponding indices in the index set S_0. In Step 5, NNCI calculates the mean value of these neighboring outcomes, $\overline{y}_i^{(0)} = \dfrac{1}{k} \sum_{j \in S_0} y_j$. Similarly, in Step 6-7, NNCI calculates the mean value of k-nearest neighbors' outcomes in treatment group (i.e $T = 1$), namely $\overline{y}_i^{(1)} = \frac{1}{k} \sum_{j \in S_1} y_j$.
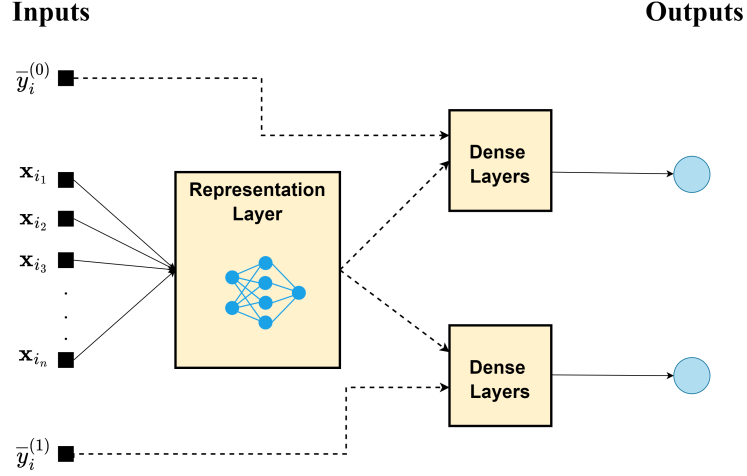
Inputs   **Outputs**

Figure 1: Example of the application of NNCI methodology to a neural network model

Algorithm 1: NNCI

Inputs:

    k: number of nearest neighbors

    $\mathbf{X}$: covariate matrix

    $\mathbf{t}$: vector of treatment values t

    $\mathbf{y}$: vector of outcome values y

Outputs:

    $\overline{\mathbf{y}}^{(0)}$: vector with average of k-nearest outcomes from control group for each sample

    $\overline{\mathbf{y}}^{(1)}$: vector with average of k-nearest outcomes from treatment group for each sample

Step 1: Set $\overline{\mathbf{y}}^{(0)} = \mathbf{0}$ and $\overline{\mathbf{y}}^{(1)} = \mathbf{0}$

Step 2: for $i = 1$ **to** n **do**

Step 3: $\mathbf{x}_i = \mathbf{X}[i, :]$

Step 4:   Calculate the index set S_0 containing the indices of the k-nearest neighbors of $\mathbf{x}_i$ with $T = 0$

Step 5: $\overline{y}_i^{(0)} = \dfrac{1}{k} \displaystyle\sum_{j \in S_0} y_j$

Step 6:   Calculate the index set S_1 containing the indices of the k-nearest neighbors of $\mathbf{x}_i$ with $T = 1$

Step 7: $\overline{y}_i^{(1)} = \dfrac{1}{k} \displaystyle\sum_{j \in S_1} y_j$

Step 8: end

Step 9: Return $\overline{\mathbf{y}}^{(0)}, \overline{\mathbf{y}}^{(1)}$.

Based on this iterative process, NNCI calculates the average outcomes from control and treated groups and store these quantities into $\overline{\mathbf{y}}^{(0)}$ and $\overline{\mathbf{y}}^{(1)}$, respectively. These vectors are then used in conjuction with Dragonnet, TARnet and

NEDnet models for the prediction of conditional outcomes $Q(t, \mathbf{x}) = E(Y \mid X = \mathbf{x}, T = t)$ and propensity score $g(x) = P(T = 1 \mid X = \mathbf{x})$, which measures the probability of a subject to belong in the treatment group, based on its characteristics. The computational complexity for calculating the vectors $\overline{\mathbf{y}}^{(0)}$ and $\overline{\mathbf{y}}^{(1)}$ is $O(n^2)$, where n is the number of training instances. This implies that for large datasets, the computational cost may generally be considered high. In these cases, one can use a sub-sampling strategy, where only a randomly selected subset of the training set is considered for the estimation of vectors $\overline{\mathbf{y}}^{(0)}$ and $\overline{\mathbf{y}}^{(1)}$ and the cost would be $O(m \cdot n)$, where $m << n$ is the number of samples used for the estimation.

3.2.1 NN-Dragonnet

Next, we present the NN-Dragonnet model, which is based on the adoption of the NNCI methodology in the state-of-the-art Dragonnet model Shi et al. (2019). The inputs of NN-Dragonnet model are the instance $\mathbf{x}_i$, the average outcomes of its k neighboring instances from the control group $\overline{y}_i^{(0)}$ and the average outcomes of its k neighboring instances from the treatment group $\overline{y}_i^{(1)}$. The outputs of the proposed model are the predictions of the conditional outcomes $\hat{Q}(0, \mathbf{x}_i, \overline{y}_i^{(0)}; \theta)$ and $\hat{Q}(1, \mathbf{x}_i, \overline{y}_i^{(1)}; \theta)$ and the prediction of the propensity score $\hat{g}(\mathbf{x}_i; \theta)$, where θ is the vector with the network's parameters. These are computed from the model's three-head architecture.

Figure 2 illustrates the architecture of the proposed NN-Dragonnet model. Initially, the instance $\mathbf{x}_i$ is processed by three dense layers of 200 neurons each, with Exponential Linear Unit (ELU) activation function for producing the representation layer $Z(\mathbf{x}_i) \in \mathbb{R}^p$. Then, $Z(\mathbf{x}_i)$ is concatenated with $\overline{y}_i^{(0)}$ and processed by two dense layers of 100 neurons with ELU activation function and kernel regularizer of 10^{-2}. Next, an output layer of one neuron with linear activation provides the prediction of the outcome $\hat{Q}(0, \mathbf{x}_i, \overline{y}_i^{(0)}; \theta)$.

Similarly, $Z(\mathbf{x}_i)$ is concatenated with $\overline{y}^{(1)}$ and processed by two dense layers of 100 neurons with ELU activation function and kernel regularizer of 10^{-2} and a linear output for providing the prediction of the outcome $\hat{Q}(1, \mathbf{x}_i, \overline{y}_i^{(1)}; \theta)$. Furthermore, $Z(\mathbf{x}_i)$ is used for providing the prediction for the propensity score $\hat{g}(\mathbf{x}_i; \theta)$, using linear activation followed by a sigmoid.
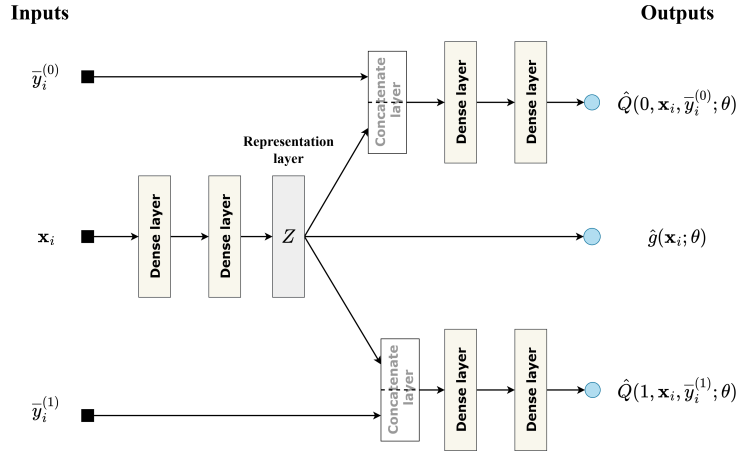

Figure 2: NN-Dragonnet architecture

The NN-Dragonnet model is trained using the following loss, which is a modification of *targeted regularization* Shi et al. (2019), namely:

$$
\begin{aligned}
\hat{\theta}, \hat{\epsilon} \;=\; & \underset{\theta, \epsilon}{\arg\min} \left[\hat{R}\left(\theta; \mathbf{X}, \overline{\mathbf{y}}^{(0)}, \overline{\mathbf{y}}^{(1)}\right) \right. \\
& \left. + \;\; \beta \frac{1}{n} \sum_i \gamma\left(y_i, t_i, \mathbf{x}_i, \overline{\mathbf{y}}_i^{(0)}, \overline{\mathbf{y}}_i^{(1)}; \theta, \epsilon\right) \right]
\end{aligned}
\tag{4}
$$

where $\beta > 0$ and $\epsilon > 0$ are hyper-parameters and

$$
\begin{aligned}
\hat{R}(\theta; \mathbf{X}, \overline{\mathbf{y}}^{(0)}, \overline{\mathbf{y}}^{(1)}) \quad = \quad & \frac{1}{n} \sum_i \left[\left(\hat{Q}\left(t_i, \mathbf{x}_i, \overline{\mathbf{y}}_i^{(0)}, \overline{\mathbf{y}}_i^{(1)}; \theta\right) - y_i \right)^2 \right. \\
& \left. + \quad \alpha f(\hat{g}(\mathbf{x}_i; \theta), t_i) \right]
\end{aligned} \tag{5}
$$

and

$$
\begin{aligned}
\gamma(y_i, t_i, \mathbf{x}_i, \overline{\mathbf{y}}^{(0)}, \overline{\mathbf{y}}^{(1)}; \theta, \epsilon) \quad = \quad & \left(y_i - \tilde{Q}\left(t_i, \mathbf{x}_i, \overline{\mathbf{y}}^{(0)}, \overline{\mathbf{y}}^{(1)}; \theta, \epsilon\right) \right)^2 \\
\tilde{Q}(t_i, \mathbf{x}_i, \overline{\mathbf{y}}^{(0)}, \overline{\mathbf{y}}^{(1)}; \theta, \epsilon) \quad = \quad & \hat{Q}\left(t_i, \mathbf{x}_i, \overline{\mathbf{y}}^{(0)}, \overline{\mathbf{y}}^{(1)}; \theta\right) \\
& + \quad \epsilon \left[\frac{t_i}{\hat{g}(\mathbf{x}_i; \theta)} - \frac{1 - t_i}{1 - \hat{g}(\mathbf{x}_i; \theta)} \right]
\end{aligned}
$$

3.2.2 NN-TARnet

We present the NN-TARnet model, which is based on the adoption of NNCI methodology in the TARnet model. The inputs are the instances $\mathbf{x}_i$, the average outcomes of its k neighboring instances from control group $\overline{y}_i^{(0)}$ and the average outcomes of its k neighboring instances from treatment group $\overline{y}_i^{(1)}$; while the outputs are the conditional outcomes for the two different groups of subjects, control $\hat{Q}(0, \mathbf{x}_i, \overline{y}_i^{(0)}; \theta)$ and treatment $\hat{Q}(1, \mathbf{x}_i, \overline{y}_i^{(1)}; \theta)$ groups, where θ is the vector with the network's parameters.

Figure 3 presents the architecture of NN-TARnet neural network model. As regards to NN-TARnet model, $\mathbf{x}_i$ is processed by three dense layers of 200 neurons with ELU activation function and the representation layer $Z(\mathbf{x}_i) \in \mathbb{R}^p$ is produced.

Next, $Z(\mathbf{x}_i)$ is concatenated with $\overline{y}_i^{(0)}$ and processed by two dense layers of 100 neurons with ELU activation function and kernel regularizer of 10^{-2}. Next, an output layer of one neuron with linear activation provides the prediction of the outcome $\hat{Q}(0, \mathbf{x}_i, \overline{y}_i^{(0)}; \theta)$. Likewise, $Z(\mathbf{x}_i)$ is concatenated with $\overline{y}^{(1)}$ and processed by two dense layers of 100 neurons with ELU activation function and kernel regularizer of 10^{-2} and a linear output for providing the prediction of the outcome $\hat{Q}(1, \mathbf{x}_i, \overline{y}_i^{(1)}; \theta)$.
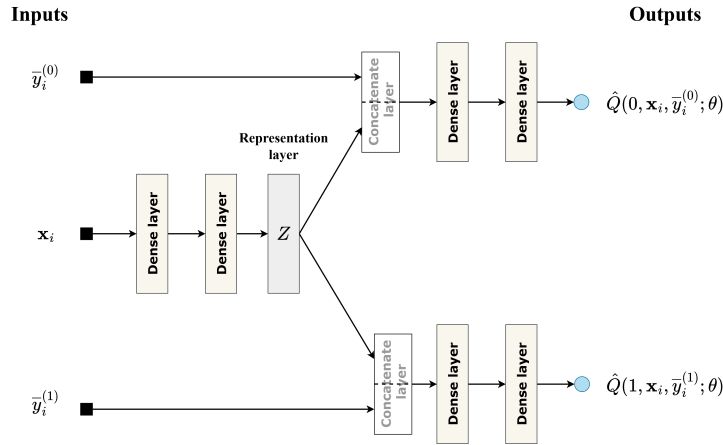

Figure 3: NN-TARnet architecture

Essentially, NN-TARnet uses the same architecture as NN-Dragonnet for the estimation of conditional outcomes, with the difference that NN-Dragonnet uses the propensity score for targeted regularization.

3.2.3 NN-NEDnet

Next, we present NN-NEDnet, a model which is based on the adoption of NNCI methodology by NEDnet. NN-NEDnet shares the same architecture with NN-Dragonnet, with the difference that it is not based on an end-to-end philosophy, but on a multi-stage procedure.

Initially, NN-NEDnet is trained utilizing a treatment prediction task (Figure 4(a)). In this case, the representation layer is trained using cross-entropy loss on the propensity score $\hat{g}(\mathbf{x}_i\,;\theta)$. Then, the conditional outcome head is removed and substituted by an outcome prediction network, similar with the one used by NN-Dragonnet (Figure 4(b)). The difference is that the representation layers are frozen and concatenated with the inputs $\overline{y}_i^{(0)}$ and $\overline{y}_i^{(1)}$ for estimating the conditional outcomes $\hat{Q}(0, \mathbf{x}_i, \overline{y}_i^{(0)}; \theta)$ and $\hat{Q}(1, \mathbf{x}_i, \overline{y}_i^{(1)}; \theta)$, respectively, where θ is the vectors of NN-NEDnet's parameters. In this case, the representation layer is frozen and the final model is frozen and trained using the mean squared error loss on the factual outcomes, i.e.,

$$\hat{\mathcal{L}}(\theta; \mathbf{X}, \overline{\mathbf{y}}^{(0)}, \overline{\mathbf{y}}^{(1)}) = \frac{1}{n} \sum_i \left[\left(\hat{Q}\left(t_i, \mathbf{x}_i, \overline{\mathbf{y}}_i^{(0)}, \overline{\mathbf{y}}_i^{(1)}; \theta\right) - y_i \right)^2 \right.$$
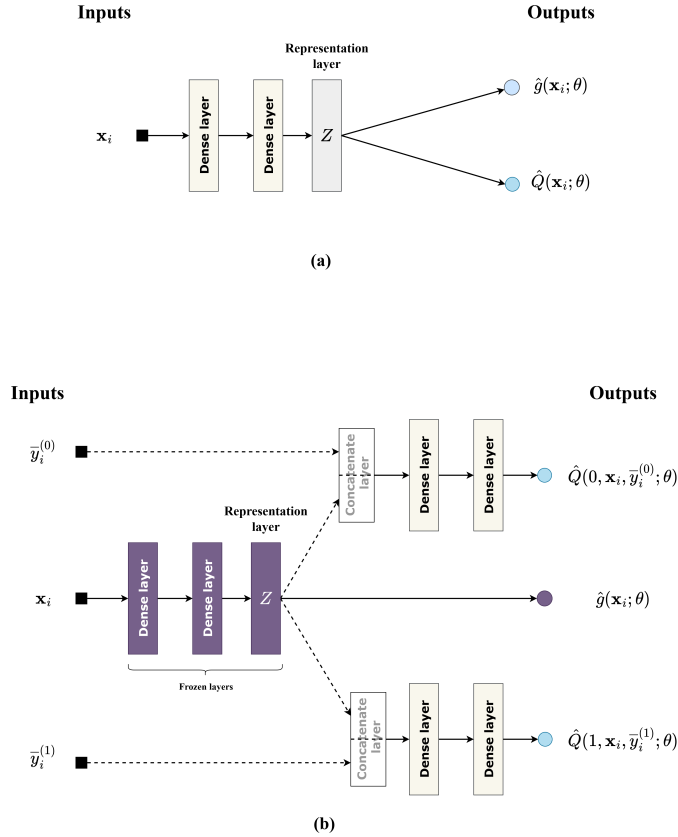

(a)

(b)

Figure 4: NN-NEDnet architecture. (a) Treatment prediction mask, used for training. (b) Outcome prediction, with frozen representation layers.

4 Evaluation Methodology & Datasets

In this section, we comprehensively describe the tools for the evaluation of causal inference models.

4.1 Performance Profiles & Statistical Analysis

The most commonly used performance metrics for evaluating the estimation of treatment effects include the absolute error in the estimation of ATE and the error of Precision in Estimation of Heterogeneous Effect (PEHE), Johansson

et al. (2016); Louizos et al. (2017); Shalit et al. (2017); Yoon et al. (2018); Kiriakidou and Diou (2022a) which are respectively defined as follows:

$$|\epsilon_{ATE}| = \left| \frac{1}{n} \sum_{i=1}^{n} (y_i^{(1)} - y_i^{(0)}) - \frac{1}{n} \sum_{i=1}^{n} (\hat{y}_i^{(1)} - \hat{y}_i^{(0)}) \right| \tag{6}$$

and

$$\epsilon_{PEHE} = \frac{1}{n} \sum_{i=1}^{n} \left((y_i^{(1)} - y_i^{(0)}) - (\hat{y}_i^{(1)} - \hat{y}_i^{(0)}) \right)^2 \tag{7}$$

where $\hat{y}_i^{(t)}$ indicates the model's outcome prediction for the i-th sample for treatment t. Notice that ϵ_{ATE} and ϵ_{PEHE} concern the evaluation of the estimation of average (ATE) and individual (ITE) treatment effects, respectively.

In the literature, it is common to use ensembles of experiments for the evaluation of the models' effectiveness which is usually carried out by calculating the average $|\epsilon_{ATE}|$ and ϵ_{PEHE} across the experiments. Nonetheless, this approach may be misleading in some cases, since all problems are equally considered for the models' evaluation and a small number of them tend to dominate the results Kiriakidou and Diou (2022b,a).

To address this problem, we adopt the evaluation framework for causal inference models proposed in Kiriakidou and Diou (2022b), using the performance profiles of Dolan and Moré Dolan and Moré (2002) and a comprehensive statistical analysis based on nonparametric and post-hoc tests. The performance profiles provide us information such as probability of success, effectiveness and robustness in compact form Livieris (2018); Livieris et al. (2020). Each profile plots the fraction P of experiments for which any given model is within a factor τ of the best model. Statistical analysis is conducted to examine the hypothesis that a pair of models perform equally well and provide statistical evidence about the superiority of the proposed model Fernández et al. (2017); Livieris et al. (2019); Livieris and Pintelas (2020); Vuttipittayamongkol and Elyan (2020); Tampakas et al. (2019). Firstly, we apply the non-parametric Friedman Aligned-Ranks (FAR) test Hodges Jr and Lehmann (1962) to rank the evaluated models from the best to the worst performance and the Finner post-hoc test Finner (1993) to examine whether there are statistically significant differences among the evaluated models' performance.

4.2 Datasets

The fundamental problem of causal inference is that in practice, we only have access to the factual outcomes, which prohibits model evaluation. To address this issue, we used simulated or semi-synthetic datasets, which include both outcomes for each sample. It is worth mentioning that the selected datasets are the most widely used in the field of causal inference and have been chosen by various researchers Yao et al. (2018); Shi et al. (2019); Johansson et al. (2016); Shalit et al. (2017); Louizos et al. (2017) for the evaluation of their proposed models.

IHDP dataset. It constitutes a collection of semi-simulated datasets, which was constructed from the Infant Health and Development Program Hill (2011). Each dataset is composed by 608 units in the control group and 139 units in the treatment group, while the 25 covariates are collected from a real-world randomized experiment. Furthermore, the effect of home visits by specialists was studied on future cognitive test scores. In our experiments, we used the setting "A" in NPCI package Dorie composed by 1000 realizations. Notice that 80% of the data were used for training the models, while the rest 20% was used for testing.

Synthetic dataset. It consists of a collection of toy datasets, which was originally introduced by Louizos et al. Louizos et al. (2017). Its generation is based on the hidden confounder variable W using the following process:

$$
\begin{aligned}
w_i &\sim & \text{Bern}(0.5) \\
t_i \,|\, w_i &\sim & \text{Bern}(0.75 w_i + 0.25(1 - w_i)) \\
x_i \,|\, w_i &\sim & \mathcal{N}(w_i, \sigma_{z_1}^2 w_i + \sigma_{z_0}^2 (1 - w_i)) \\
y_i \,|\, t_i, w_i &\sim & \text{Bern}(\text{Sigmoid}(3(w_i + 2(2t_i - 1))))
\end{aligned}
$$

,where Sigmoid is the logistic sigmoid function and $\sigma_{z_0} = 3, \sigma_{z_1} = 5$. Notice that the treatment variable T and the proxy to the confounder X constitute a mixture of Bernoulli and Gaussian distribution, respectively. Finally, 90% of the data were used for training the models, while the rest 10% was used for testing.

ACIC dataset. This dataset was developed for the *2018 Atlantic Causal Inference Conference competition data* Yishai et al. (2018). ACIC is a collection of semi-synthetic datasets, which were received from the linked birth and infant death data MacDorman and Atkinson (1998). Every competition dataset is a sample from a distinct distribution and data are generated through a generating process, by possessing different treatment selection and outcome functions.

Following Shi et al. Shi et al. (2019) for each data generating process setting, four and eight datasets were randomly picked of size 5000 and 10000, respectively. Notice that 80% of the data were used for training the models, while the rest 20% was used for testing.

5 Numerical Experiments

In this section, we evaluate the prediction performance of the neural network models, which integrate the proposed NNCI methodology against the corresponding baseline models, on IHDP, Synthetic and ACIC datasets. More specifically, we evaluate the performance of the proposed NN-Dragonnet, NN-TARnet, NN-NEDnet against Dragonnet, TARnet and NEDnet, respectively.

The implementation code was written in Python 3.7 using Tensorflow Keras library Gulli and Pal (2017) and run on a PC (3.2GHz Quad-Core processor, 16GB RAM) using Windows operating system. Notice that Dragonnet, TARnet and NEDNet were used with their default optimized parameter settings, while for the proposed models the number of neighbors was set to $k = 11$ and targeted regularization was implemented with $\alpha = 1$ and $\beta = 1$ Shalit et al. (2017).

The curves in the following figures have the following meaning

- "Dragonnet" stands for the state-of-the-art neural network-based model Dragonnet Shi et al. (2019).
- "TARnet" stands for the neural network-based model TARnet Shalit et al. (2017).
- "NEDnet" stands for the two-stage neural network-based model NEDnet Shi et al. (2019).
- "NN-Dragonnet" stands for the proposed NN-Dragonnet model, which modifies Dragonnet using the NNCI methodology.
- "NN-TARnet" stands for the NN-TARnet model, which modifies TARnet using the NNCI methodology.
- "NN-NEDnet" stands for the NN-NEDnet model, which modifies NEDnet using the NNCI methodology.

Additionally, it is worth mentioning that the proposed models were implemented using three different distance metrics i.e Euclidean, Manhattan and Chebychev as in Kiriakidou and Diou (2022a). These distances belong to the class of Minkowski distances and constitute the most widely used distances proposed in the literature Pandit et al. (2011); Singh et al. (2013).

5.1 Evaluation on IHDP dataset

Figure 5 presents the performance profiles of NN-Dragonnet, NN-TARnet, NN-NEDnet and their corresponding baseline models Dragonnet, TARnet and NEDnet, based on the performance metrics $|\epsilon_{ATE}|$ and ϵ_{PEHE}. All versions of NN-Dragonnet exhibit similar performance with state-of-the-art Dragonnet in terms of $|\epsilon_{ATE}|$, while they considerably outperform Dragonnet in terms of ϵ_{PEHE}. Additionally, the adoption of NNCI methodology considerably improved the performance of TARnet model, relative to both performance metrics since the curves of all versions of NN-TARnet lie on the top. NN-NEDnet solves almost the same percentage of benchmarks with the best (lowest) $|\epsilon_{ATE}|$ for any used distance metric and outperforms the baseline model NN-NEDnet model in terms of robustness. Finally, it is worth mentioning that all proposed models exhibited similar performance using any distance metric. In detail all versions of NN-NEDnet outperform the baseline model since their curves lie on the top.

Tables 1 and 2 present the statistical analysis of the proposed causal inference models and their corresponding baseline models for IHDP dataset, in terms of $|\epsilon_{ATE}|$ and ϵ_{PEHE}, respectively. As regards $|\epsilon_{ATE}|$, Dragonnet model reports the best rank according to FAR test. However, Finner post-hoc test suggests that there are no statistically significant differences in the performance between Dragonnet and all versions of NN-Dragonnet model, which implies that all models perform similarly. NN-TARnet and NN-NEDnet report the highest probability-based ranking, outperforming TARnet and NEDnet, respectively. Additionally, Finner post-hoc test suggests that there are statistically significant differences in the performance between all versions of both NN-TARnet and NN-NEDnet with their corresponding baseline models. As regards ϵ_{PEHE} performance metric, the interpretation of Table 2 reveals that NN-Dragonnet, NN-TARnet and NN-NEDnet are the top ranking models, outperforming the baseline models, Dragonnet, TARnet and NEDnet, respectively. Therefore, we able to conclude that we obtained strong statistical evidence that the adoption of the NNCI methodology considerably improved the performance of all baseline causal inference models.
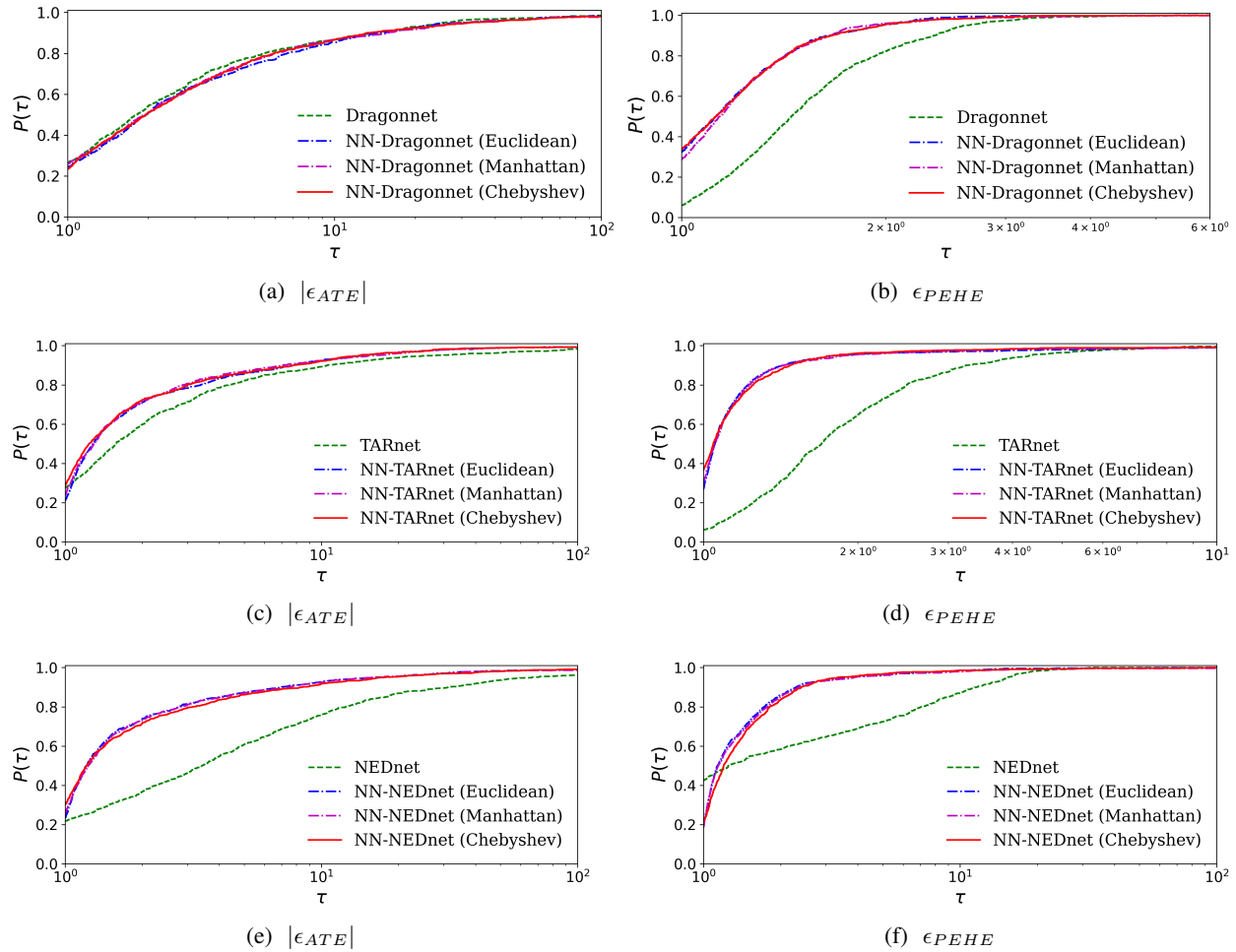
Figure 5: Log_{10} Performance profiles of models, based on $|\epsilon_{ATE}|$ and ϵ_{PEHE} for IHDP dataset

Table 1: FAR test and Finner post-hoc test based on $|\epsilon_{ATE}|$ for IHDP dataset

Model	FAR	Finner post-hoc test	
		p_F-value	H_0
Dragonnet	1840.19	-	-
NN-Dragonnet (Manhattan)	1894.39	0.282160	Fail to reject
NN-Dragonnet (Chebyshev)	1935.42	0.094191	Fail to reject
NN-Dragonnet (Euclidean)	1947.98	0.094191	Fail to reject
NN-TARnet (Manhattan)	1827.99	-	-
NN-TARnet (Chebyshev)	1831.38	0.947642	Fail to reject
NN-TARnet (Euclidean)	1872.75	0.519053	Fail to reject
TARnet	2469.86	0.000000	Reject
NN-NEDnet (Manhattan)	1839.56	-	-
NN-NEDnet (Chebyshev)	1845.91	0.938142	Fail to reject
NN-NEDnet (Euclidean)	1849.75	0.938142	Fail to reject
NEDnet	2457.28	0.000000	Reject

Table 2: FAR test and Finner post-hoc test based on ϵ_{PEHE} for IHDP dataset

Model	FAR	Finner post-hoc test	
		p_F-value	H_0
NN-Dragonnet (Euclidean)	1628.32	-	-
NN-Dragonnet (Manhattan)	1653.07	0.623290	Fail to reject
NN-Dragonnet (Chebyshev)	1670.39	0.539643	Fail to reject
Dragonnet	2666.19	0.000000	Reject
NN-TARnet (Euclidean)	1609.48	-	-
NN-TARnet (Manhattan)	1624.02	0.86625	Fail to reject
NN-TARnet (Chebyshev)	1626.72	0.86625	Fail to reject
TARnet	3141.77	0.000000	Reject
NN-NEDnet (Euclidean)	1908.98	-	-
NN-NEDnet (Manhattan)	1937.97	0.574488	Fail to reject
NN-NEDnet (Chebyshev)	2001.56	0.107503	Fail to reject
NEDnet	2150.38	0.000000	Reject

5.2 Evaluation on Synthetic dataset

Figure 6 demonstrates the performance profiles of the proposed NN-Dragonnet, NN-TARnet, NN-NEDnet and their corresponding state-of-the-art models Dragonnet, TARnet and NEDnet, in terms of $|\epsilon_{ATE}|$ and ϵ_{PEHE} performance metrics. Firstly, relative to $|\epsilon_{ATE}|$ all versions of the proposed models report almost identical performance while the use of Euclidean distance presents slightly better performance. NN-Dragonnet's versions exhibited similar performance with Dragonnet while NN-TARnet's and NN-NEDnet's versions slightly outperform the traditional TARnet and NEDnet, respectively in terms of efficiency. In case of ϵ_{PEHE}, NN-Dragonnet and NN-NEDnet outperformed Dragonnet and NEDnet, respectively using any distance metric since their curves lie on the top. In detail, all versions of both NN-Dragonnet and NN-NEDnet presented the highest percentage of simulations with the best (lowest) ϵ_{PEHE}. In contrast, NN-TARnet and TARnet reported almost identical performance, independent of the utilized distance metric.

Tables 3 presents the statistical analysis for the proposed causal inference models and their corresponding baseline models for Synthetic dataset, in terms of $|\epsilon_{ATE}|$. NN-Dragonnet (Manhattan) is the top ranking model since it presents the best (lowest) FAR score. Nevertheless, Finner post-hoc tests suggests that there is no statistically significant differences in the performance of all evaluated models. NN-TARnet and NN-NEDnet present the highest FAR ranking using the Euclidean distance. Additionally, Finner post-hoc test suggests that there exist significant differences between the performance of the proposed NN-TARnet and NN-NEDnet and the corresponding baseline models TARnet and NEDnet, independent of the utilized distance metrics. This implies that the adoption of the proposed NNCI methodology benefit the TARnet and NEDnet in terms of $|\epsilon_{ATE}|$.
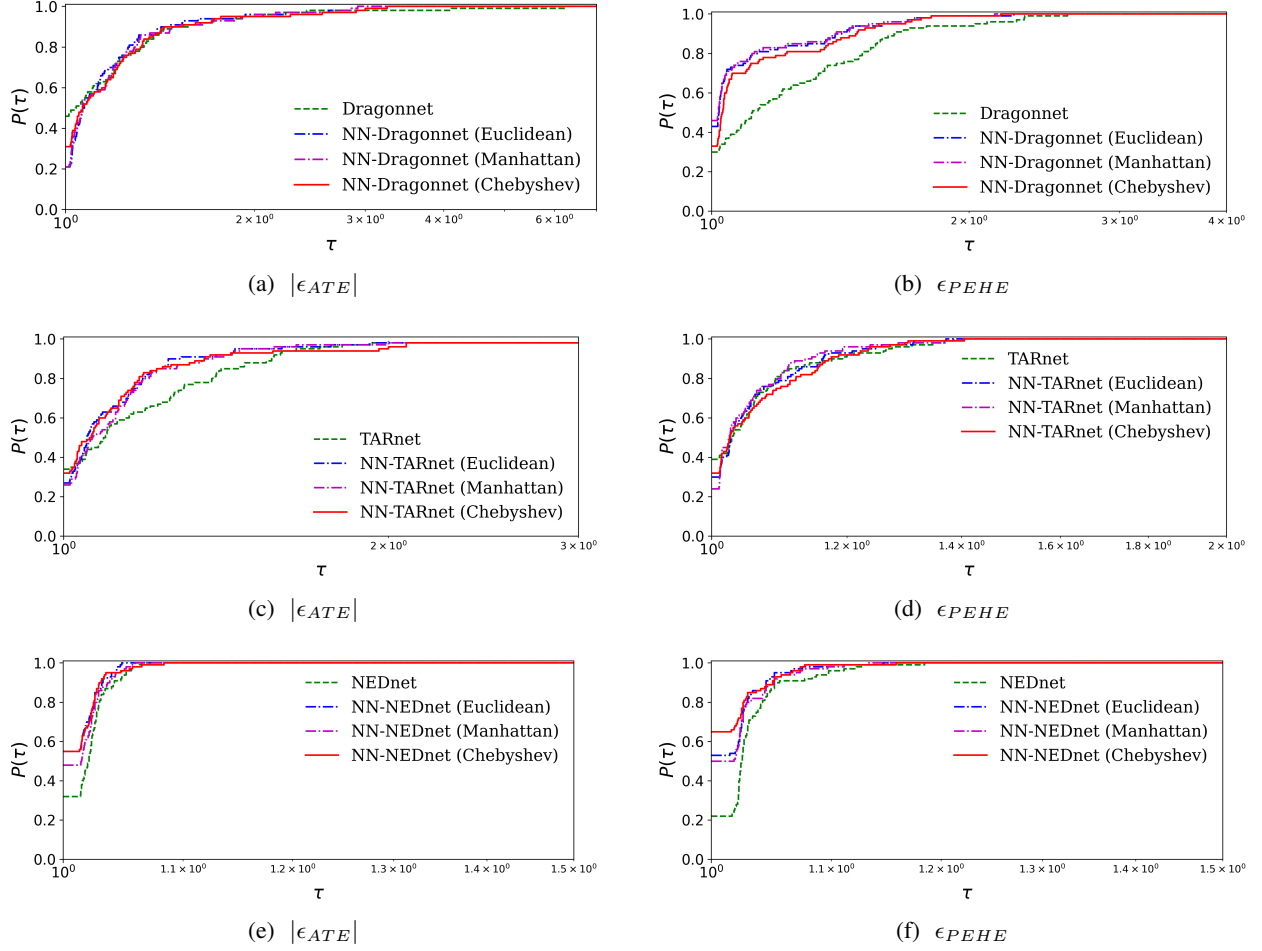
Figure 6: Log_{10} Performance profiles of models, based on $|\epsilon_{ATE}|$ and ϵ_{PEHE} for Synthetic dataset

Tables 4 presents the statistical analysis for the proposed causal inference models and their corresponding baseline models for Synthetic dataset, in terms of ϵ_{PEHE}. Both statistical tests provide statistical evidence that the proposed NN-Dragonnet and NN-NEDnet outperformed Dragonnet and NEDnet, respectively and are able to exhibit more reliable predictions. In contrast, although NN-TARnet present higher ranking than TARnet, there are no statistically significant differences in their performance, relative to ϵ_{PEHE} metric.

5.3 Evaluation on ACIC dataset

Figure 7 presents the performance profiles of NN-Dragonnet, NN-TARnet, NN-NEDnet and their corresponding baseline models, for $|\epsilon_{ATE}|$ and ϵ_{PEHE} performance metrics. NN-Dragonnet outperform the state-of-the-art Dragonnet model independent of the used distance metric as regards both performance metrics. Additionally, it reported slightly better performance in case the Manhattan distance metric is used for the calculation of the neighboring instances. NN-TARnet (Chebyshev) model exhibits the best overall performance, slightly outperforming the rest of the models, relative to $|\epsilon_{ATE}|$, while NN-TARnet (Manhattan) reports the best performance, relative to ϵ_{PEHE}. NN-NEDnet (Chebyshev) exhibits the highest probability of being the optimal model in terms of effectiveness and robustness, since its curves lies on the top for both performance metrics. More specifically, NN-NEDnet solved 50% and 66% of the simulations with the best (lowest) $|\epsilon_{ATE}|$ and ϵ_{PEHE} scores, while NEDnet reported only 23% and 24% in the same cases.

Tables 5 and 6 present the statistical analysis for the proposed causal inference models and their corresponding baseline models for ACIC dataset, in terms of $|\epsilon_{ATE}|$ and ϵ_{PEHE}, respectively. NN-Dragonnet (Manhattan) is the top ranking model relative to both performance metrics. FAR and Finner post-hoc tests suggests that NN-Dragonnet outperforms the baseline Dragonnet and there exhist statistically significant differences in their performances. Additionally, NN-

Table 3: FAR test and Finner post-hoc test based on $|\epsilon_{ATE}|$ for Synthetic dataset

Model	FAR	Finner post-hoc test	
		p_F-value	H_0
NN-Dragonnet (Manhattan)	198.31	-	-
Dragonnet	200.89	0.994708	Fail to reject
NN-Dragonnet (Chebyshev)	200.89	0.994708	Fail to reject
NN-Dragonnet (Euclidean)	201.91	0.994708	Fail to reject
NN-TARnet (Euclidean)	186.43	-	-
NN-TARnet (Manhattan)	190.16	0.841249	Fail to reject
NN-TARnet (Chebyshev)	192.58	0.841249	Fail to reject
TARnet	232.83	0.013568	Reject
NN-NEDnet (Euclidean)	175.99	-	-
NN-NEDnet (Chebyshev)	182.04	0.711365	Fail to reject
NN-NEDnet (Manhattan)	191.46	0.468763	Fail to reject
NEDnet	252.51	0.000009	Reject

Table 4: FAR test and Finner post-hoc test based on ϵ_{PEHE} for IHDP dataset

Model	FAR	Finner post-hoc test	
		p_F-value	H_0
NN-Dragonnet (Manhattan)	173.37	-	-
NN-Dragonnet (Euclidean)	177.45	0.802946	Fail to reject
NN-Dragonnet (Chebyshev)	193.46	0.310031	Fail to reject
Dragonnet	257.72	0.000000	Reject
NN-TARnet (Manhattan)	190.71	-	-
NN-TARnet (Euclidean)	199.64	0.630507	Fail to reject
TARnet	202.13	0.630507	Fail to reject
NN-TARnet (Chebyshev)	209.51	0.578490	Fail to reject
NN-NEDnet (Chebyshev)	155.34	-	-
NN-NEDnet (Euclidean)	172.58	0.291693	Fail to reject
NN-NEDnet (Manhattan)	190.71	0.0045430	Reject
NEDnet	283.37	0.000000	Reject

Dragonnet presents the best performance in case the Manhattan distance is utilized. Non-parametric FAR statistical test presents that NN-TARnet presents higher ranking compared to TARnet relative to both performance metrics; nevertheless, the Finner post-hoc test suggests that for all versions of NN-TARnet model there are no statistically significant differences in their performance. Finally, the interpretation of Tables 5 and 6 suggest that NN-NEDnet presented slightly higher ranking than the baseline model NEDnet.

Summarizing, we point out that the proposed methodology significantly improved the performance of the baseline models in case of imbalanced datasets (IHDP), which indicates that the proposed approach is more beneficial to challenging and complex benchmarks. This issue should be further taken into consideration and analysis in order to study why and how the proposed NNIC methodology improves the prediction accuracy especially in case of imbalanced problems.

6 Discussion

In this section, we provide a comprehensive discussion about the motivation and contribution of this work as well as about the advantages of the proposed NNCI methodology and its limitations.

In a recent work, Kiriakidou and Diou Kiriakidou and Diou (2022a) proposed a new approach of modifying the state-of-the-art causal inference model Dragonnet by enriching the model's inputs with the average outcomes of the k-nearest neighbor samples from control and treatment groups. Furthermore, the authors presented some promising
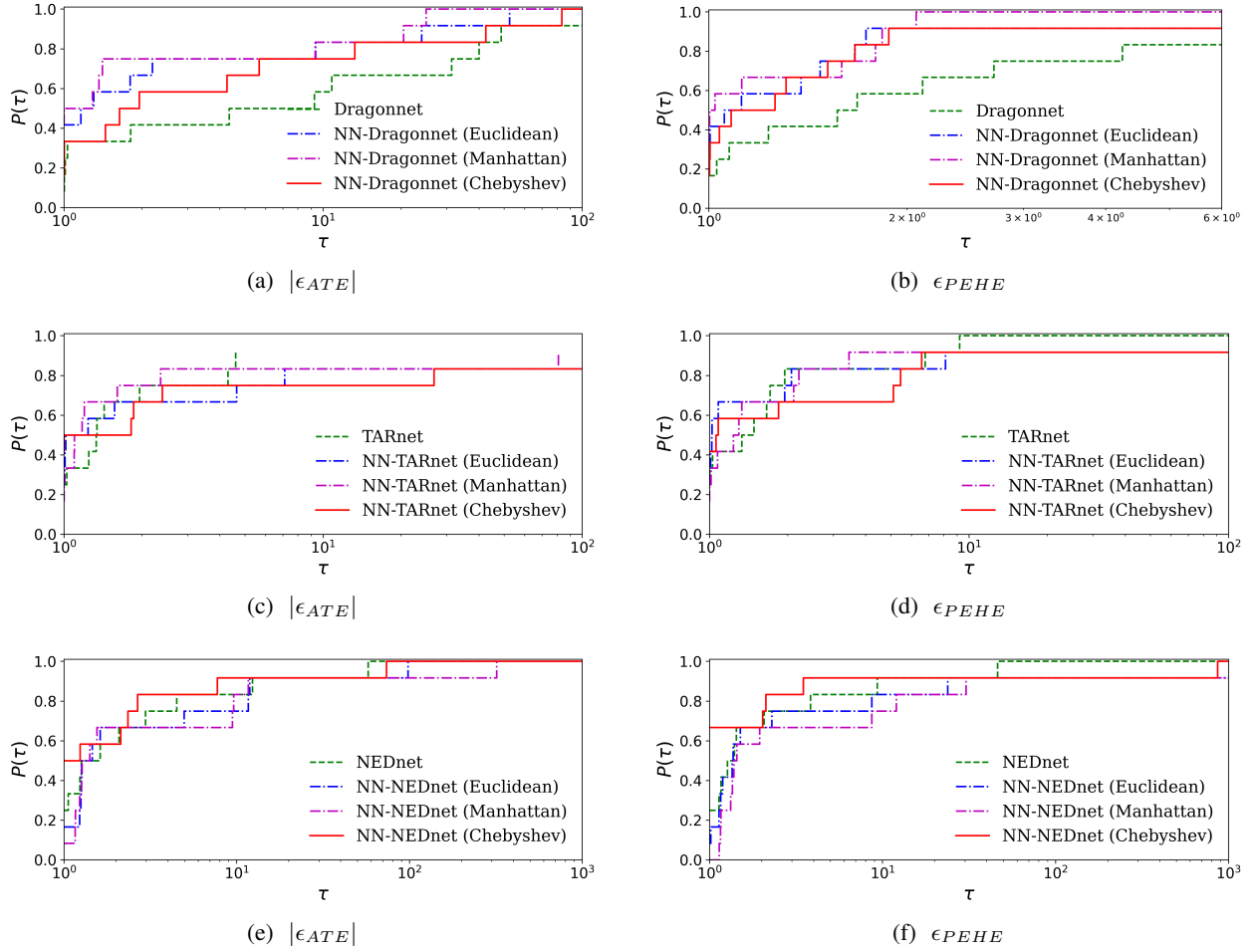
(a) $|\epsilon_{ATE}|$

(b) ϵ_{PEHE}

(c) $|\epsilon_{ATE}|$

(d) ϵ_{PEHE}

(e) $|\epsilon_{ATE}|$

(f) ϵ_{PEHE}

Figure 7: Log_{10} Performance profiles of models, based on $|\epsilon_{ATE}|$ and ϵ_{PEHE} for ACIC dataset

numerical experiments using the IHDP dataset, which revealed the efficiency of their approach. However, the major drawbacks of this work were that the authors adopted the proposed approach only on Dragonnet and evaluated the performance of the proposed model only on one causal inference benchmark.

Motivated by the efficiency of their approach and the promising experimental results, we extend the work conducted in Kiriakidou and Diou (2022a) and address their major drawbacks. In this research, we propose NNCI methodology for integrating valuable information from the nearest neighboring samples from control and treatment groups in the training data, which is then utilized as inputs in the neural network models to provide accurate predictions of average and individual treatment effects. The proposed NNCI methodology is then integrated to the most effective neural network-based causal inference models i.e. Dragonnet, TARnet and NEDnet. These models use a deep net to produce a representation layer, which is then processed independently for predicting both the outcomes for treatment and control groups.

The presented numerical experiments reveal that the application of NNCI considerably improve the performance of the state-of-the-art neural network models, achieving better estimation of both average and individual treatment effects. The evaluation was performed using three of the most well-known causal inference benchmarks i.e. IHDP, Synthetic and ACIC, which are characterized by high complexity and challenge. The performance profiles as well as the Friedman Aligned-Ranks and Finner post-hoc tests provide strong statistical evidence about the effectiveness of the proposed approach. Therefore, based on this experimental analysis, we conclude that the proposed NNCI methodology in conjunction with modified versions of Dragonnet, TARnet and NEDnet is able to accurately estimate treatment effects. In more detail, as regards IHDP dataset, the proposed causal inference models outperformed the corresponding traditional ones for both $|\epsilon_{ATE}|$ and ϵ_{PEHE}, independent of the utilized distance metric. It is worth mentioning that IHDP is an imbalanced dataset, which indicates that NNCI methodology proved beneficial for challenging and complex

Table 5: FAR test and Finner post-hoc test based on $|\epsilon_{ATE}|$ for ACIC dataset

Model	FAR	Finner post-hoc test	
		p_F-value	H_0
NN-Dragonnet (Manhattan)	18.25	-	-
NN-Dragonnet (Euclidean)	22.33	0.474959	Fail to reject
NN-Dragonnet (Chebyshev)	26.58	0.209181	Fail to reject
Dragonnet	30.83	0.080796	Reject
NN-TARnet (Chebyshev)	20.91	-	-
NN-TARnet (Manhattan)	22.75	0.812511	Fail to reject
NN-TARnet (Euclidean)	23.33	0.812511	Fail to reject
TARnet	31.00	0.215446	Fail to reject
NN-NEDnet (Chebyshev)	22.16	-	-
NN-NEDnet (Euclidean)	23.25	0.849667	Fail to reject
NN-NEDnet (Manhattan)	25.41	0.763596	Fail to reject
NEDnet	27.16	0.763596	Fail to reject

Table 6: FAR test and Finner post-hoc test based on ϵ_{PEHE} for ACIC dataset

Model	FAR	Finner post-hoc test	
		p_F-value	H_0
NN-Dragonnet (Manhattan)	19.25	-	-
NN-Dragonnet (Euclidean)	21.75	0.661815	Fail to reject
NN-Dragonnet (Chebyshev)	23.58	0.590268	Fail to reject
Dragonnet	33.41	0.039045	Reject
NN-TARnet (Manhattan)	20.75	-	-
NN-TARnet (Euclidean)	22.41	0.770588	Fail to reject
NN-TARnet (Chebyshev)	24.58	0.649006	Fail to reject
TARnet	30.25	0.262418	Fail to reject
NN-NEDnet (Chebyshev)	16.66	-	-
NN-NEDnet (Euclidean)	23.58	0.226216	Fail to reject
NEDnet	28.16	0.069785	Fail to reject
NN-NEDnet (Manhattan)	29.58	0.069785	Fail to reject

benchmarks. Concerning the Synthetic dataset, the experimental analysis reveals that the proposed models presented the best overall performance in case the Manhattan distance was used. Finally, regarding ACIC dataset, the adoption of the proposed NNCI methodology to the state-of-the-art causal inference models improved the average treatment effect estimation.

It is worth mentioning that NNCI methodology can be adopted only to the selected neural network based causal inference models due to their special architecture design. More specifically, NNCI assumes the existence of a representation layer prior to the final treatment effect estimation layers. This can be considered as a limitation of the proposed work. Therefore, the adoption of the proposed methodology to other causal inference models models is an interesting research direction for future work.

7 Conclusion

In this work, we proposed a new methodology, named NNCI, which is applied to well-established neural network-based models for the estimation of individual (ITE) and average treatment effects (ATE). An advantage of the proposed methodology is the exploitation of valuable information, not only from the covariates, but also from the outcomes of nearest neighboring instances contained in the training data from both treatment and control group. The proposed NNCI methodology is applied to the state-of-the-art neural network models, Dragonnet, NEDnet and TARnet, aiming to increase the models' prediction accuracy and reduce bias.

The experimental analysis on three widely used datasets in the field of causal inference, illustrated that the proposed approach improved the performance of the traditional neural network-based models, regarding the estimation of causal effects. This is confirmed by the performance profiles of Dolan and Moré as well as the nonparametric FAR test and the post-hoc Finner test. It is worth highlighting that in all of the cases the proposed methodology leads to considerable improvement in the estimation of treatment effects, in terms of effectiveness and robustness.

Nevertheless, a limitation of the proposed work is the selection of the distance metric used for calculating the nearest neighbors as well as the optimal value of parameter k. An evaluation study on the effectiveness and sensitivity of different values of parameter k and distance metrics is included as future work. Another promising research subject can be considered the use of dynamic ensemble learning algorithms Alam et al. (2020); Pintelas and Livieris (2020); Nandi et al. (2022); Ortiz et al. (2016), finite element machine learning Amezquita-Sancheza and Valtierra-Rodriguez (2020); Pereira et al. (2020) and self-supervised learning Rafiei et al. (2022); Hua et al. (2022) for further improving the prediction performance. Finally, an interesting idea for achieving more accurate predictions of causal effects is the development of new models for causal inference based on the architecture of augmented machine learning models Bhattacharya et al. (2022); Wu et al. (2022); Zhang et al. (2022a,b).

Aknowledgements

References

Sebastian Schneeweiss, Jeremy A Rassen, Robert J Glynn, Jerry Avorn, Helen Mogun, and M Alan Brookhart. High-dimensional propensity score adjustment in studies of treatment effects using health care claims data. *Epidemiology (Cambridge, Mass.)*, 20(4):512, 2009.

Shuhan Zheng, Zhichao Liang, Youzhi Qu, Qingyuan Wu, Haiyan Wu, and Quanying Liu. Kuramoto model-based analysis reveals oxytocin effects on brain network dynamics. *International Journal of Neural Systems*, 32(02): 2250002, 2022.

Philip Oreopoulos. Estimating average and local average treatment effects of education when compulsory schooling laws really matter. *American Economic Review*, 96(1):152–175, 2006.

Daniel Zantedeschi, Eleanor McDonnell Feit, and Eric T Bradlow. Measuring multichannel advertising response. *Management Science*, 63(8):2706–2728, 2017.

Kun Kuang, Lian Li, Zhi Geng, Lei Xu, Kun Zhang, Beishui Liao, Huaxin Huang, Peng Ding, Wang Miao, and Zhichao Jiang. Causal inference. *Engineering*, 6(3):253–263, 2020.

Gemma Hammerton and Marcus R Munafò. Causal inference with observational data: the need for triangulation of evidence. *Psychological medicine*, 51(4):563–578, 2021.

Claudia Shi, David Blei, and Victor Veitch. Adapting neural networks for the estimation of treatment effects. *Advances in neural information processing systems*, 32, 2019.

Uri Shalit, Fredrik D. Johansson, and David Sontag. Estimating individual treatment effect: Generalization bounds and algorithms. In *Proceedings of the 34th International Conference on Machine Learning - Volume 70*, ICML'17, page 3076–3085, Sydney, NSW, Australia, 2017. JMLR.org.

Elizabeth D Dolan and Jorge J Moré. Benchmarking optimization software with performance profiles. *Mathematical programming*, 91(2):201–213, 2002.

Helmut Finner. On a monotonicity problem in step-down multiple test procedures. *Journal of the American Statistical Association*, 88(423):920–923, 1993.

Joseph L Hodges Jr and Erich L Lehmann. Rank methods for combination of independent experiments in analysis of variance. *The Annals of Mathematical Statistics*, 33(2):482–497, 1962.

Jinsung Yoon, James Jordon, and Mihaela van der Schaar. GANITE: estimation of individualized treatment effects using generative adversarial nets. In *6th International Conference on Learning Representations, ICLR 2018, Vancouver, BC, Canada, April 30 - May 3, 2018, Conference Track Proceedings*. OpenReview.net, 2018. URL https://openreview.net/forum?id=ByKWUeWA-.

Sören R Künzel, Jasjeet S Sekhon, Peter J Bickel, and Bin Yu. Metalearners for estimating heterogeneous treatment effects using machine learning. *Proceedings of the national academy of sciences*, 116(10):4156–4165, 2019.

Hugh A Chipman, Edward I George, and Robert E McCulloch. BART: bayesian additive regression trees. *The Annals of Applied Statistics*, 4(1):266–298, 2010.

Leo Breiman. Random forests. *Machine learning*, 45(1):5–32, 2001.

Stefan Wager and Susan Athey. Estimation and inference of heterogeneous treatment effects using random forests. *Journal of the American Statistical Association*, 113(523):1228–1242, 2018.

Christos Louizos, Uri Shalit, Joris M Mooij, David Sontag, Richard Zemel, and Max Welling. Causal effect inference with deep latent-variable models. *Advances in neural information processing systems*, 30, 2017.

Arthur Gretton, Karsten M Borgwardt, Malte J Rasch, Bernhard Schölkopf, and Alexander Smola. A kernel two-sample test. *The Journal of Machine Learning Research*, 13(1):723–773, 2012.

Cédric Villani. *Optimal transport: old and new*, volume 338. Springer, 2009.

Niki Kiriakidou and Christos Diou. An improved neural network model for treatment effect estimation. In *IFIP International Conference on Artificial Intelligence Applications and Innovations*, pages 147–158. Springer, 2022a.

Jennifer L Hill. Bayesian nonparametric modeling for causal inference. *Journal of Computational and Graphical Statistics*, 20(1):217–240, 2011.

Liuyi Yao, Sheng Li, Yaliang Li, Mengdi Huai, Jing Gao, and Aidong Zhang. Representation learning for treatment effect estimation from observational data. *Advances in neural information processing systems*, 31, 2018.

Fredrik D. Johansson, Uri Shalit, and David Sontag. Learning representations for counterfactual inference. In *Proceedings of the 33rd International Conference on International Conference on Machine Learning - Volume 48*, ICML'16, page 3020–3029. JMLR.org, 2016.

Donald B Rubin. Causal inference using potential outcomes: Design, modeling, decisions. *Journal of the American Statistical Association*, 100(469):322–331, 2005.

Niki Kiriakidou and Christos Diou. An evaluation framework for comparing causal inference models. In *Proceedings of the 12th Hellenic Conference on Artificial Intelligence*, SETN '22, Corfu, Greece, 2022b. Association for Computing Machinery. ISBN 9781450395977. doi:10.1145/3549737.3549775. URL https://doi.org/10.1145/3549737.3549775.

Ioannis E Livieris. Improving the classification efficiency of an ann utilizing a new training methodology. In *Informatics*, volume 6, page 1. MDPI, 2018.

Ioannis E. Livieris, Emmanuel Pintelas, Niki Kiriakidou, and Stavros Stavroyiannis. An advanced deep learning model for short-term forecasting U.S. natural gas price and movement. In Ilias Maglogiannis, Lazaros Iliadis, and Elias Pimenidis, editors, *Artificial Intelligence Applications and Innovations. AIAI 2020 IFIP WG 12.5 International Workshops*, pages 165–176, Cham, 2020. Springer International Publishing. ISBN 978-3-030-49190-1.

Alberto Fernández, Cristobal José Carmona, Maria Jose del Jesus, and Francisco Herrera. A pareto-based ensemble with feature and instance selection for learning from multi-class imbalanced datasets. *International Journal of Neural Systems*, 27(06):1750028, 2017.

Ioannis E Livieris, Niki Kiriakidou, Andreas Kanavos, Gerasimos Vonitsanos, and Vassilis Tampakas. Employing constrained neural networks for forecasting new product's sales increase. In *Artificial Intelligence Applications and Innovations*, pages 161–172. Springer, 2019.

Ioannis E Livieris and Panagiotis Pintelas. An improved weight-constrained neural network training algorithm. *Neural Computing and Applications*, 32:4177–4185, 2020.

Pattaramon Vuttipittayamongkol and Eyad Elyan. Improved overlap-based undersampling for imbalanced dataset classification with application to epilepsy and Parkinson's disease. *International Journal of Neural Systems*, 30(08): 2050043, 2020.

Vassilis Tampakas, Ioannis E Livieris, Emmanuel Pintelas, Nikos Karacapilidis, and Panagiotis Pintelas. Prediction of students' graduation time using a two-level classification algorithm. In *Technology and Innovation in Learning, Teaching and Education: First International Conference, TECH-EDU 2018, Thessaloniki, Greece, June 20–22, 2018, Revised Selected Papers 1*, pages 553–565. Springer, 2019.

Vincent Dorie. NPCI: Non-parametrics for causal inference. URL https://github.com/vdorie/npci.

Shimoni Yishai, Yanover Chen, Karavani Ehud, and Goldschmidt Yaara. Benchmarking framework for performance-evaluation of causal inference analysis. *CoRR*, abs/1802.05046, 2018. URL http://arxiv.org/abs/1802.05046.

Marian F MacDorman and Jonnae O Atkinson. Infant mortality statistics from the linked birth/infant death data set–1995 period data. 46(6 Suppl 2):1–22, 1998.

Antonio Gulli and Sujit Pal. *Deep learning with Keras*. Packt Publishing Ltd, 2017.

Shraddha Pandit, Suchita Gupta, et al. A comparative study on distance measuring approaches for clustering. *International Journal of Research in Computer Science*, 2(1):29–31, 2011.

Archana Singh, Avantika Yadav, and Ajay Rana. k-means with three different distance metrics. *International Journal of Computer Applications*, 67(10), 2013.

Kazi Md Rokibul Alam, Nazmul Siddique, and Hojjat Adeli. A dynamic ensemble learning algorithm for neural networks. *Neural Computing and Applications*, 32:8675–8690, 2020.

Panagiotis Pintelas and Ioannis E Livieris. Special issue on ensemble learning and applications. *Algorithms*, 13(6):140, 2020.

Arijit Nandi, Fatos Xhafa, Laia Subirats, and Santi Fort. Reward-penalty weighted ensemble for emotion state classification from multi-modal data streams. *International journal of neural systems*, pages 2250049–2250049, 2022.

Andres Ortiz, Jorge Munilla, Juan M Gorriz, and Javier Ramirez. Ensembles of deep learning architectures for the early diagnosis of the Alzheimer's disease. *International journal of neural systems*, 26(07):1650025, 2016.

JP Amezquita-Sancheza and M Valtierra-Rodriguez. Machine learning in structural engineering. *Scientia Iranica*, 27 (6):2645–2656, 2020.

Danilo R Pereira, Marco Antonio Piteri, André N Souza, João Paulo Papa, and Hojjat Adeli. FEMa: A finite element machine for fast learning. *Neural Computing and Applications*, 32:6393–6404, 2020.

Mohammad H. Rafiei, Lynne V. Gauthier, Hojjat Adeli, and Daniel Takabi. Self-supervised learning for electroencephalography. *IEEE Transactions on Neural Networks and Learning Systems*, pages 1–15, 2022. doi:10.1109/TNNLS.2022.3190448.

Yu Hua, Xin Shu, Zizhou Wang, and Lei Zhang. Uncertainty-guided voxel-level supervised contrastive learning for semi-supervised medical image segmentation. *International Journal of Neural Systems*, 32(04):2250016, 2022.

Abhijeet Bhattacharya, Tanmay Baweja, and SPK Karri. Epileptic seizure prediction using deep transformer model. *International journal of neural systems*, 32(02):2150058, 2022.

Tingfang Wu, Ferrante Neri, and Linqiang Pan. On the tuning of the computation capability of spiking neural membrane systems with communication on request. *International Journal of Neural Systems*, 32(8):2250037–2250037, 2022.

Luping Zhang, Fei Xu, Dongyang Xiao, Jianping Dong, Gexiang Zhang, and Ferrante Neri. Enzymatic numerical spiking neural membrane systems and their application in designing membrane controllers. *International Journal of Neural Systems*, pages 2250055–2250055, 2022a.

Gexiang Zhang, Xihai Zhang, Haina Rong, Prithwineel Paul, Ming Zhu, Ferrante Neri, and Yew-Soon Ong. A layered spiking neural system for classification problems. *International journal of neural systems*, 32(08):2250023, 2022b.